

Supplementary Materials for

Metals likely promoted protometabolism in early ocean alkaline hydrothermal systems

Norio Kitadai*, Ryuhei Nakamura, Masahiro Yamamoto, Ken Takai, Naohiro Yoshida, Yoshi Oono

*Corresponding author. Email: nkitadai@elsi.jp

Published 19 June 2019, *Sci. Adv.* **5**, eaav7848 (2019)

DOI: 10.1126/sciadv.aav7848

This PDF file includes:

- Fig. S1. A schematic of the electrochemical cell.
- Fig. S2. XRD patterns of FeS electrolyzed at -1.0 V versus SHE for different durations.
- Fig. S3. XRD patterns of metal sulfides before and after the 7-day electrolysis.
- Fig. S4. Total charges build up during the electrolysis.
- Fig. S5. Calibration curves for organic acids by the LC-electric conductivity detector system.
- Fig. S6. Calibration curves for NO_3^- and NO_2^- by the LC-electric conductivity detector system.
- Fig. S7. Calibration curves for amino acids and ammonia by the LC-fluorescence detector system.
- Fig. S8. Calibration curves for H_2 , CO , CH_4 , and C_2H_6 by the GC-BID detector system.
- Fig. S9. Nonenzymatic reactions in the presence of pure H_2 gas, FeCl_2 , FeS, FeS_PERM, and Fe^0 and those examined in the absence of reductant.
- Fig. S10. Analytical results of fumarate (5 mM, 1.5 ml) incubated with the FeS_PERM (100 mg) at 80°C for 2 days.
- Fig. S11. Reductive amination of four keto acids promoted by the FeS_PERM in one serum bottle.
- Fig. S12. XRD patterns of CuS electrolyzed at -0.8 and -1.0 V (versus SHE) for short durations.
- Fig. S13. XRD patterns of pure Fe^0 used in the present study.
- Fig. S14. GC chromatograms of the gas headspaces of serum bottles measured after the reduction experiments of organic/inorganic compounds.
- Table S1. Summary of the reduction experiments of organic/inorganic compounds.
- Table S2. Amounts of H_2 , CO , CH_4 , and C_2H_6 in the serum bottles (30 ml) after the reduction experiments of organic/inorganic compounds.
- Table S3. Thermodynamic data for sulfide minerals.

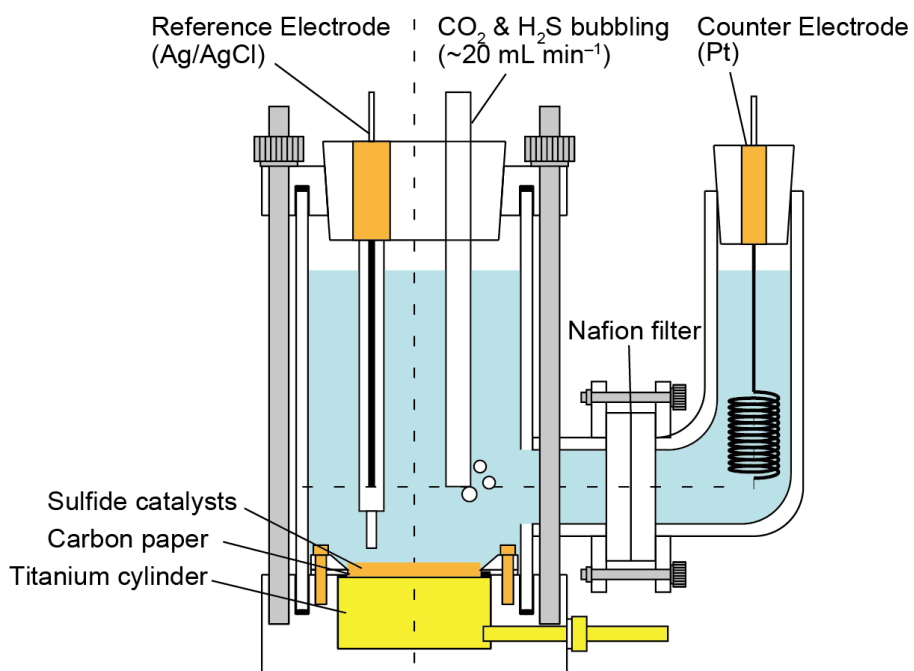


Fig. S1. A schematic of the electrochemical cell. The cell is made of a Pyrex glass tube sandwiched between a polyoxymethylene (POM) cap and basement that were tightened together with stainless screws and knurled nuts. The cell has two compartments: a large working electrode side (~100 mL) and a small counter electrode side (~15 mL) that are separated by a proton exchange membrane (Nafion 117; DuPont). On the working electrode side, a titanium cylinder (purity; 99.5%) is placed at the center of the POM basement, and is coated with carbon paper (5.7 cm²) with a silicon and POM packings. An Ag/AgCl electrode (in saturated KCl) is used as the reference, and is fixed at a distance of less than 0.5 cm from the working electrode to reduce solution resistance. On the counter side, a platinum coil is inserted into the glass tube, and is used as the counter electrode.

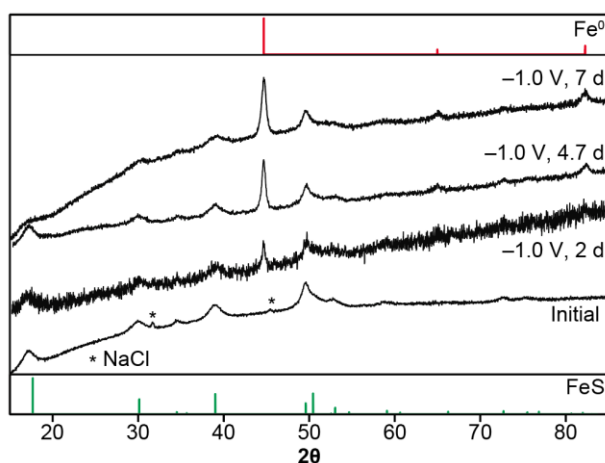


Fig. S2. XRD patterns of FeS electrolyzed at -1.0 V versus SHE for different durations.

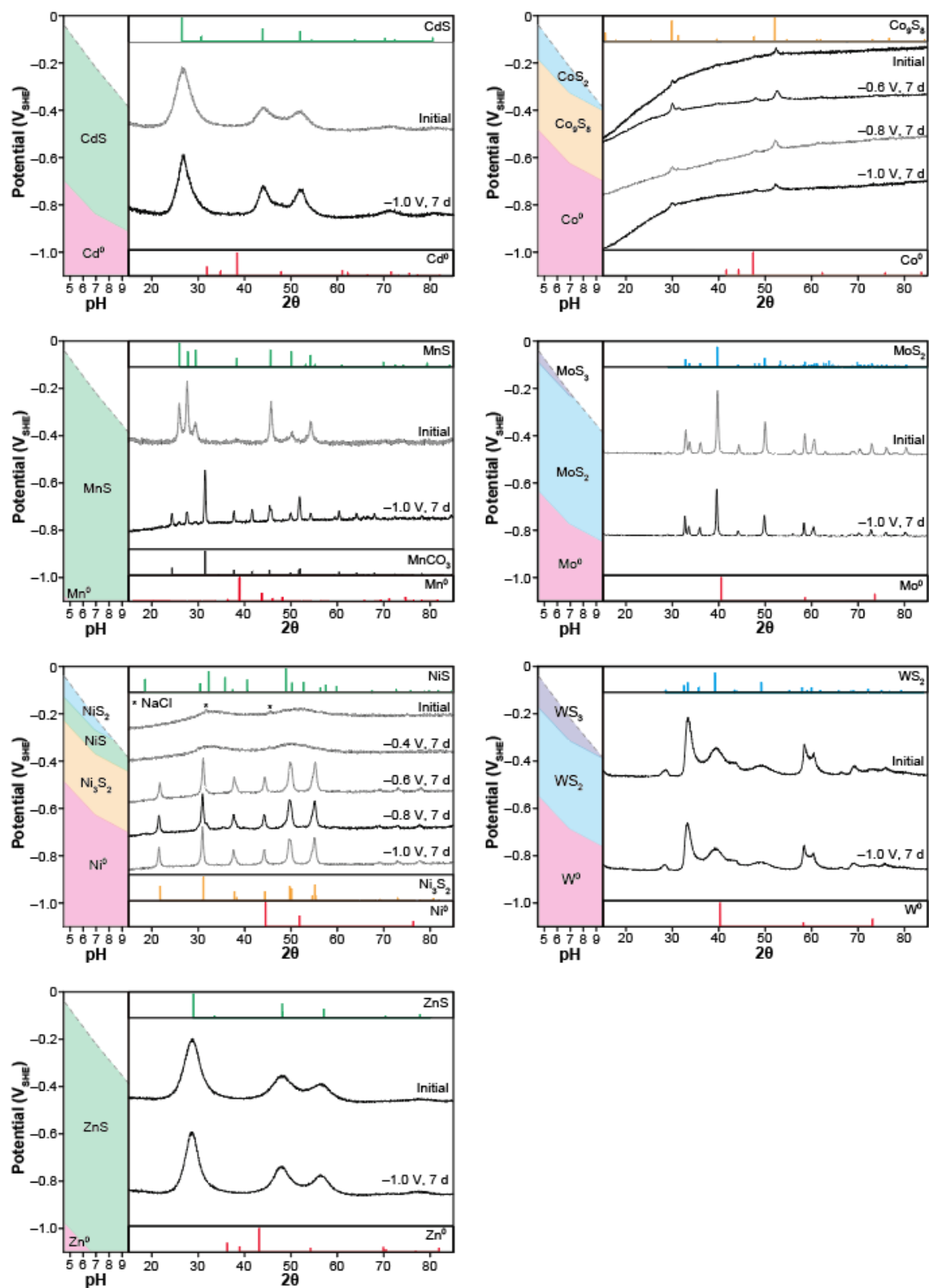


Fig. S3. XRD patterns of metal sulfides before and after the 7-day electrolysis. The color convention for the left columns is the same as that for the left columns in Fig 1B–E.

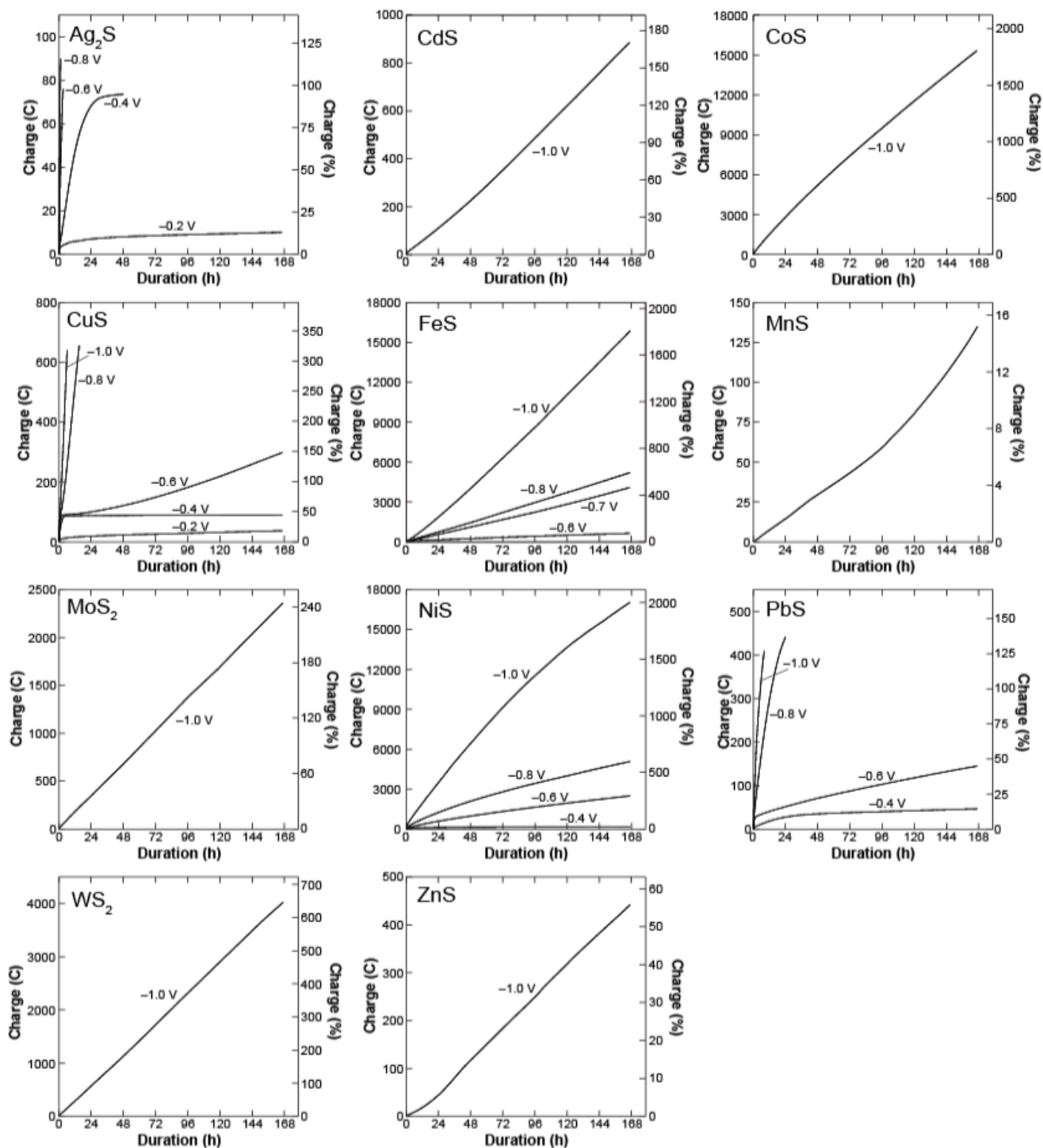


Fig. S4. Total charges build up during the electrolysis. The percentages shown at the right axis were calculated relative to the charge required for the complete sulfide-to-metal electroreduction for each reaction condition.

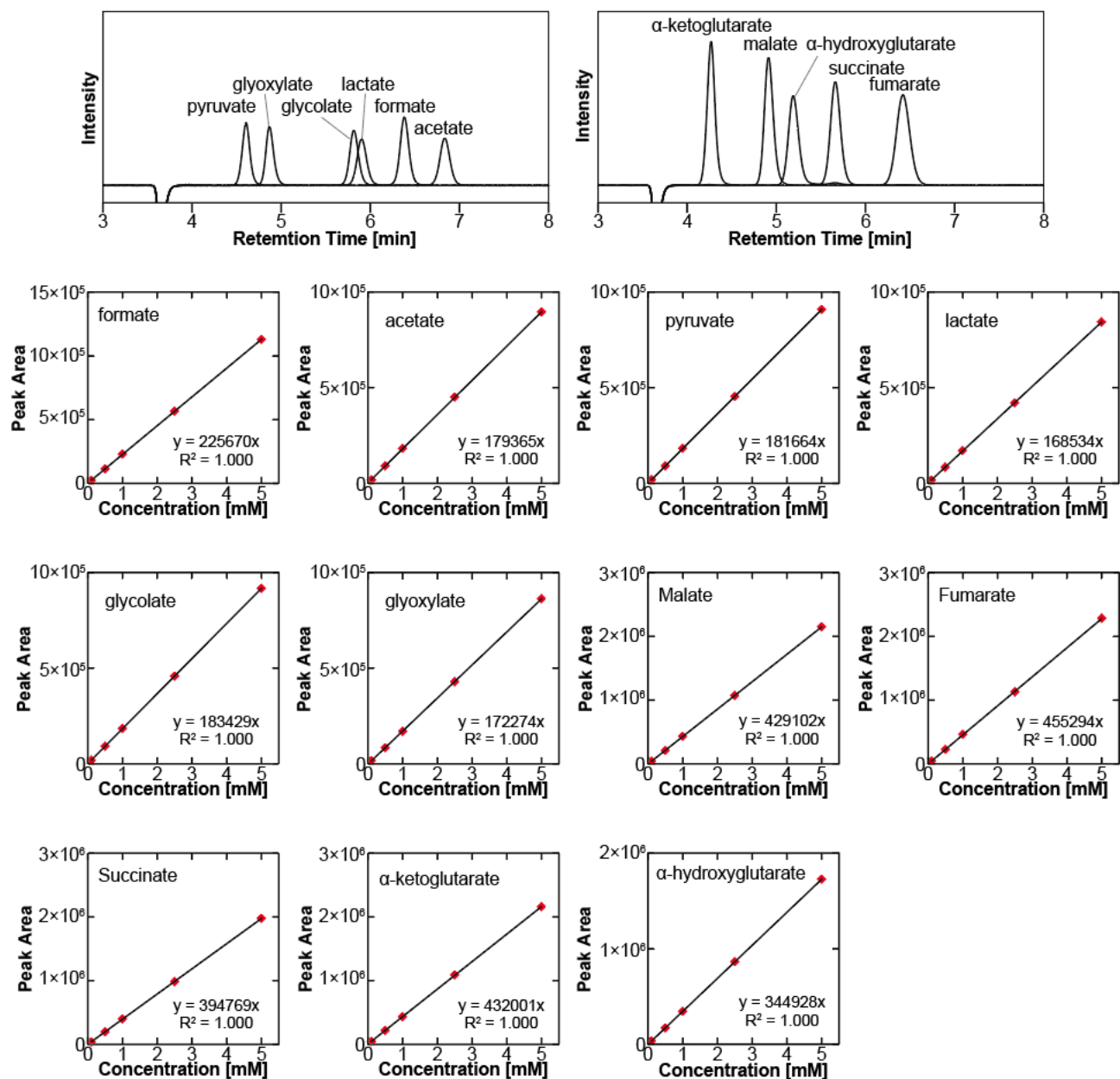


Fig. S5. Calibration curves for organic acids by the LC-electric conductivity detector system.

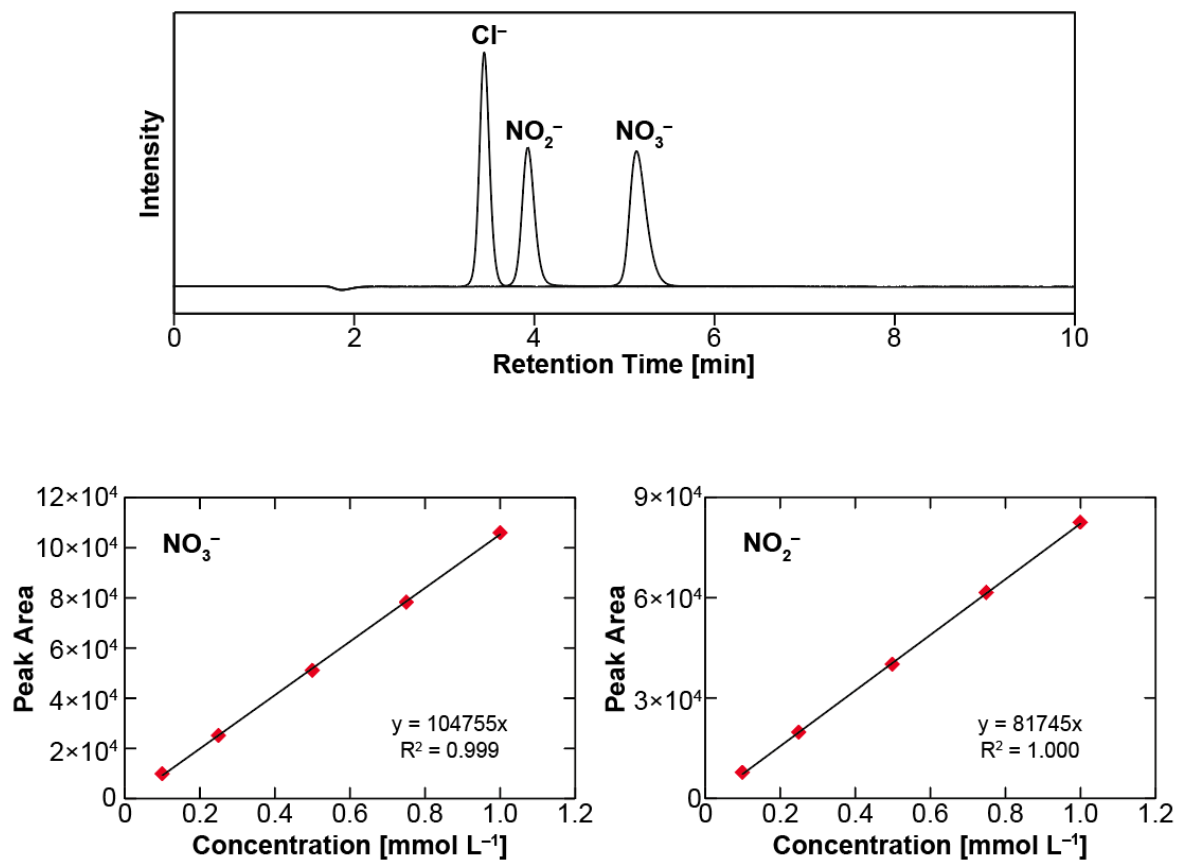


Fig. S6. Calibration curves for NO₃⁻ and NO₂⁻ by the LC-electric conductivity detector system.

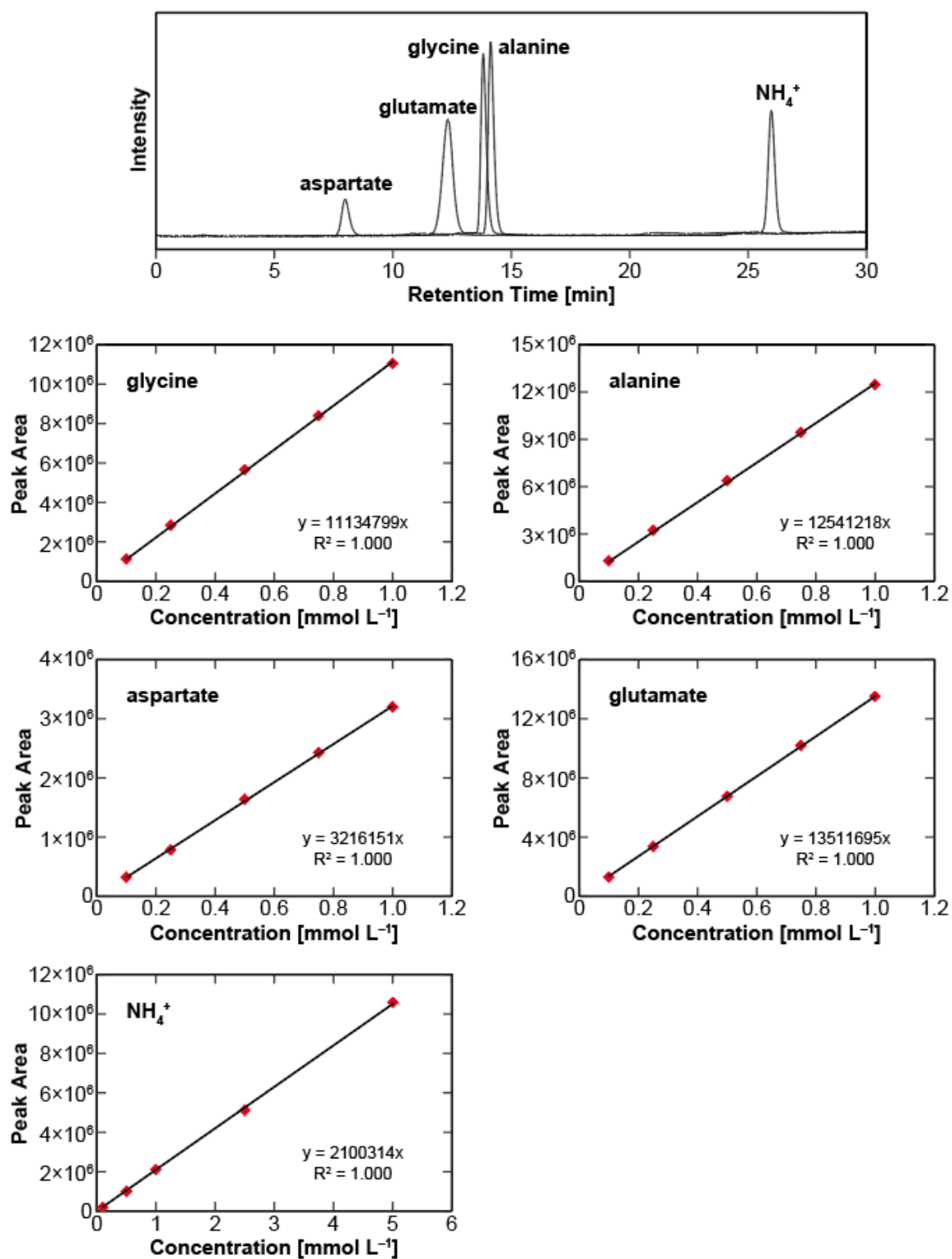


Fig. S7. Calibration curves for amino acids and ammonia by the LC-fluorescence detector system.

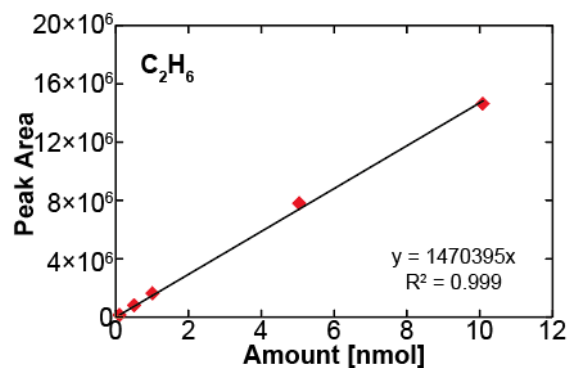
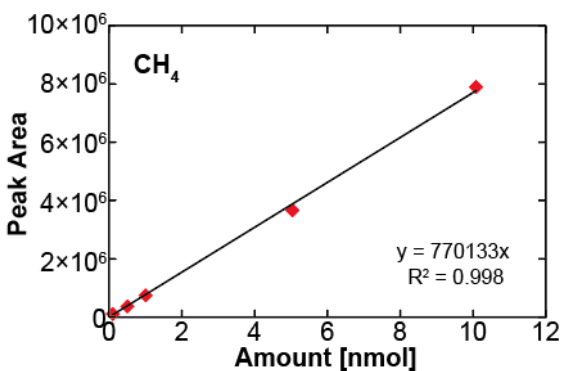
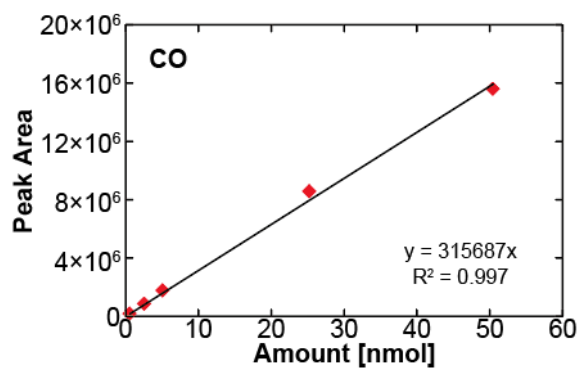
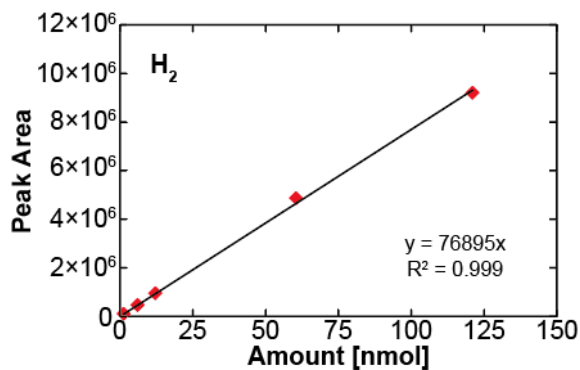
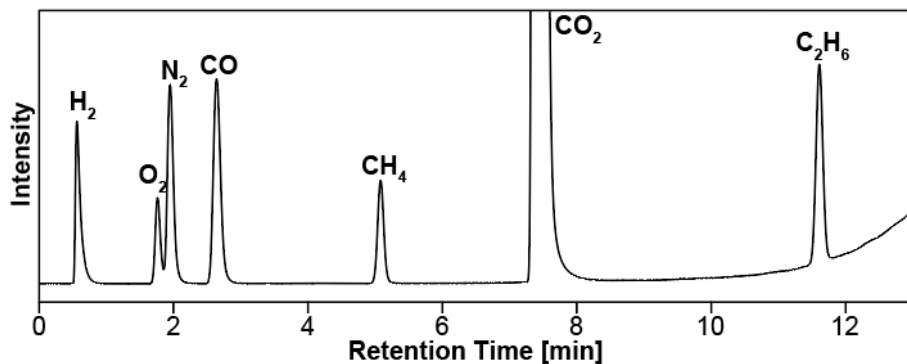


Fig. S8. Calibration curves for H₂, CO, CH₄, and C₂H₆ by the GC-BID (Barrier Ionization Discharge) detector system.

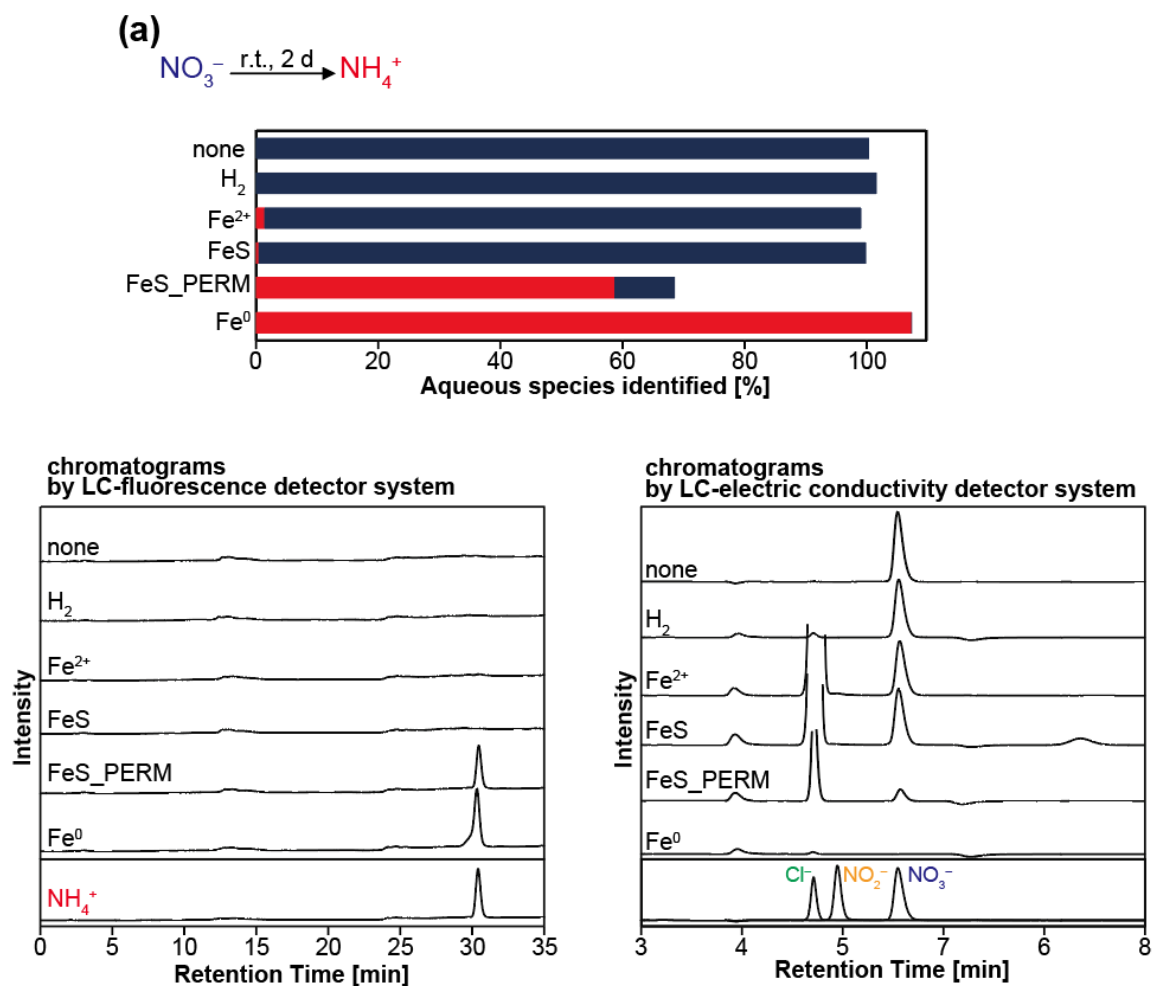


Fig. S9. Nonenzymatic reactions in the presence of pure H₂ gas, FeCl₂, FeS, FeS_PERM, and Fe⁰ and those examined in the absence of reductant. ¹H NMR spectra and chromatograms of sample products are shown with those of the standards relevant to the respective reactions. For clarity, ¹H NMR spectra are presented after deleting residual suppressed water signal around 4.8 ppm. An intense ¹H NMR signal around 4.2 ppm seen in the spectra of glyoxylate samples (**d**) are due to a glyoxylate oligomer formed in the presence of ammonia catalyst at alkaline pH (A. Hoefnagel, H. van Bekkum, J. A. Peters, The reaction of glyoxylic acid with ammonia revisited. *J. Org. Chem.* **57**, 3916–3921 (1992)).

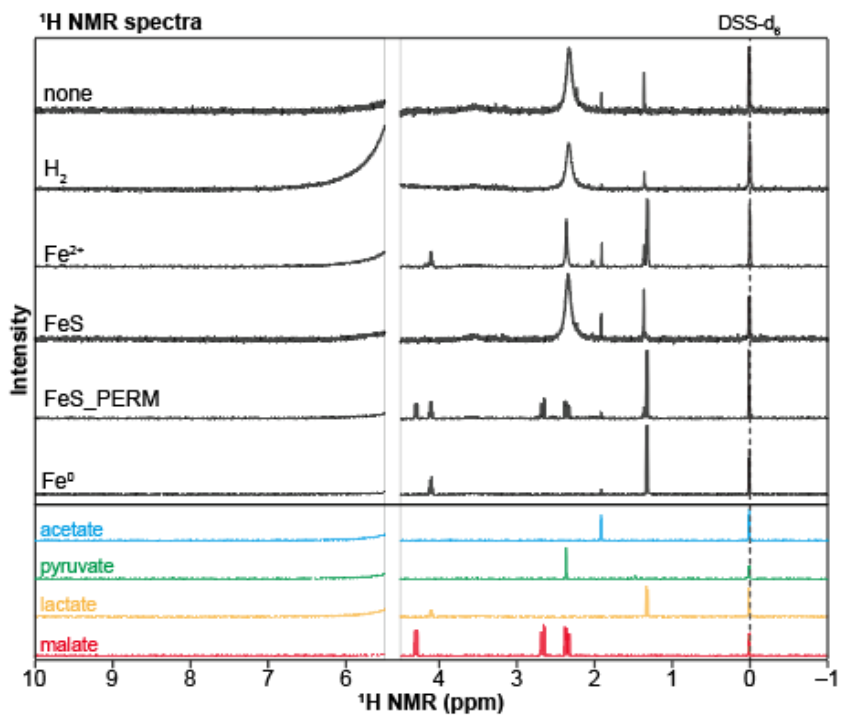
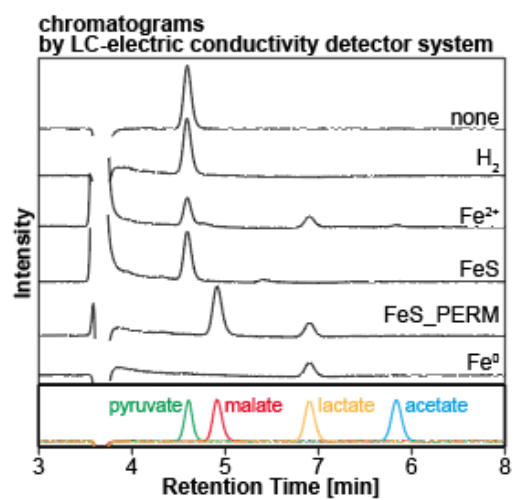
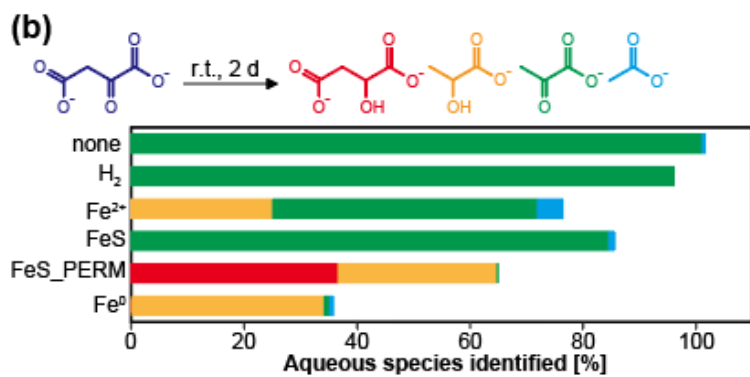


Fig. S9. (continued)

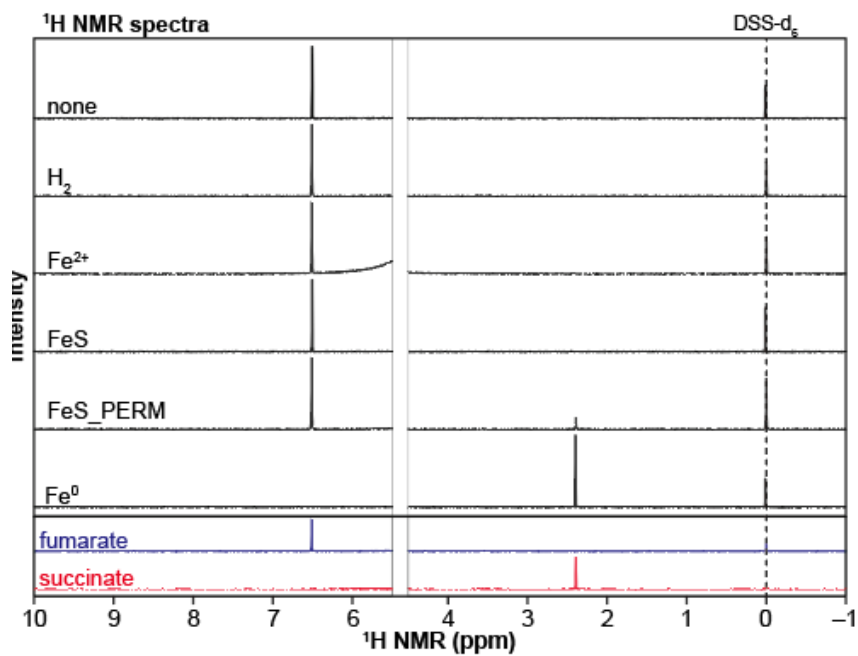
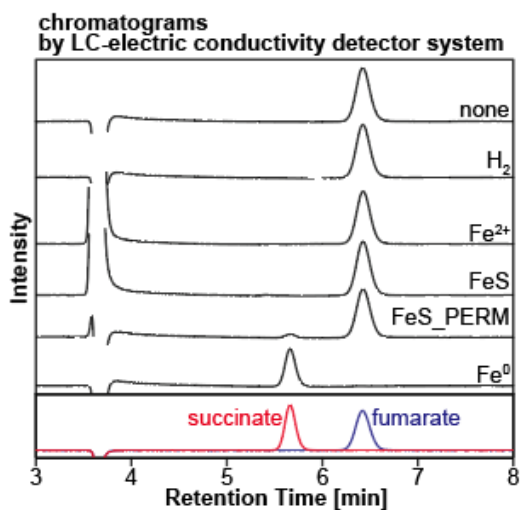
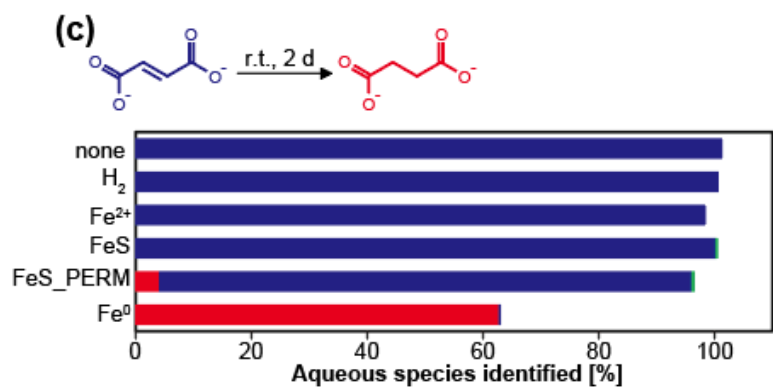


Fig. S9. (continued)

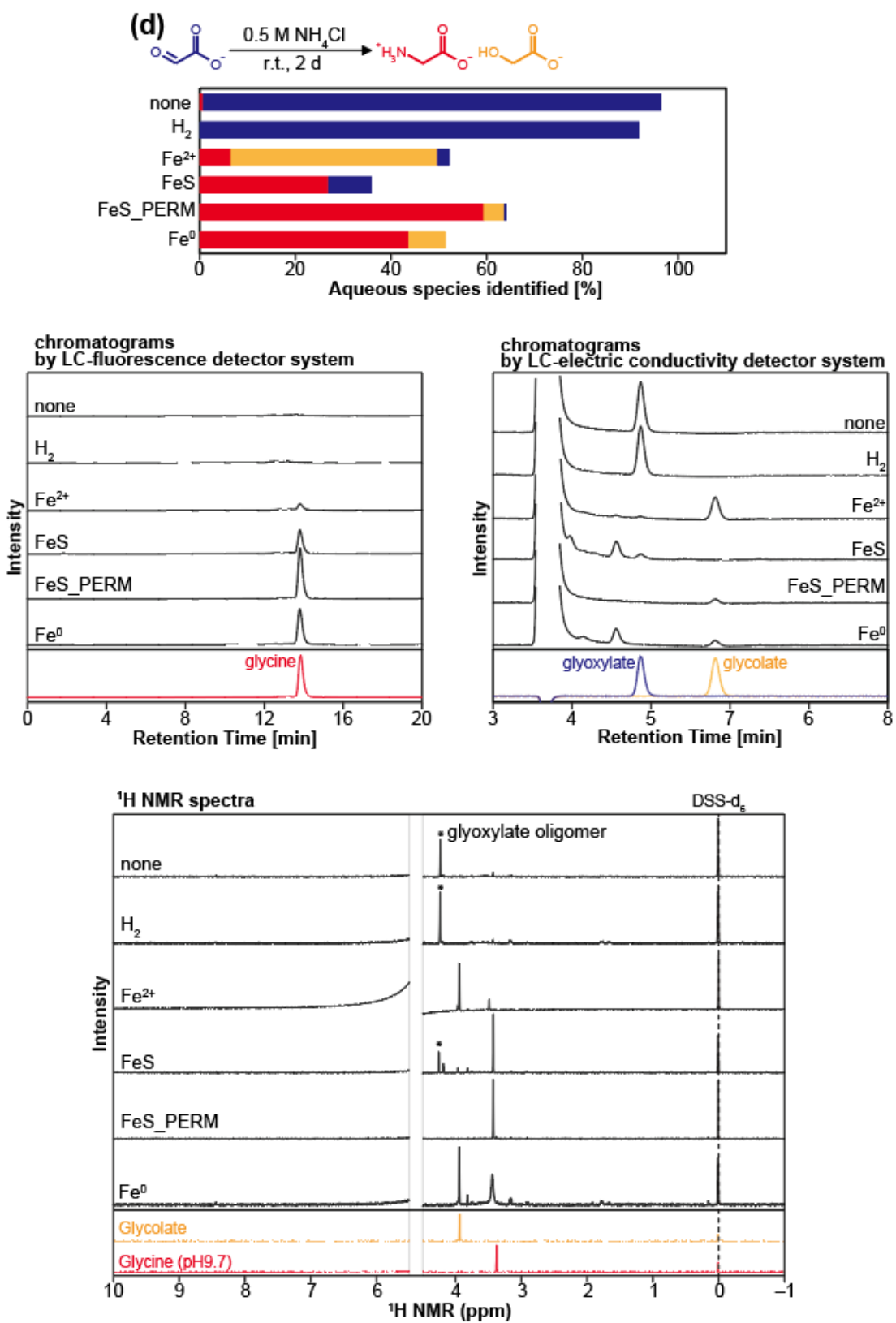


Fig. S9. (continued)

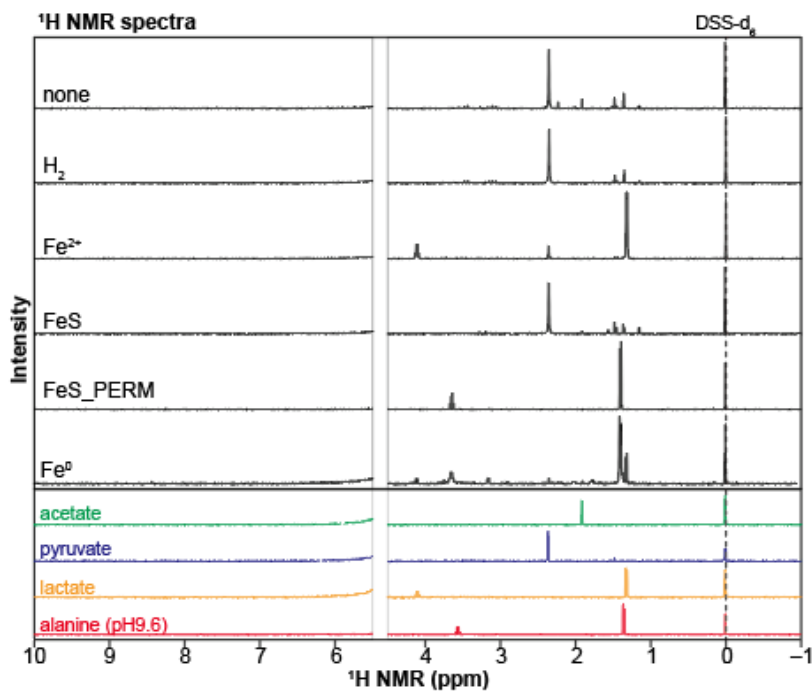
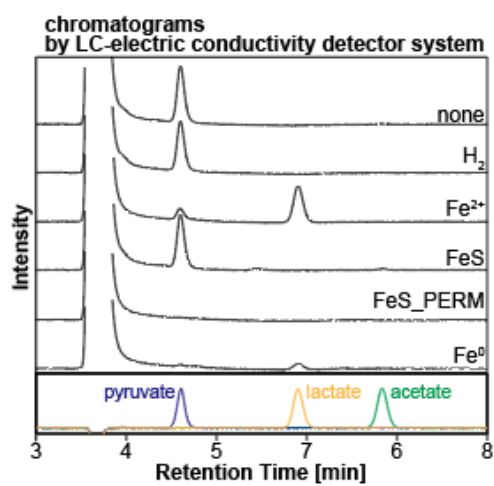
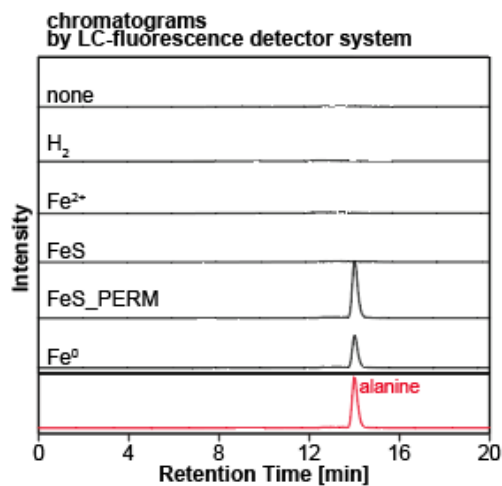
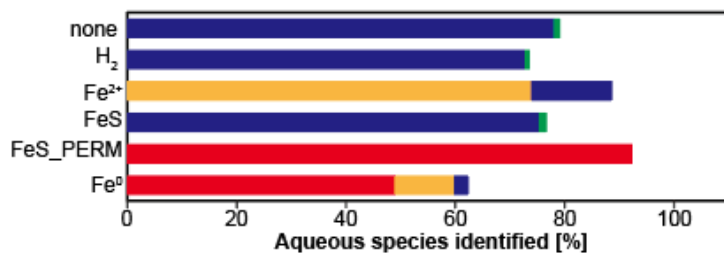
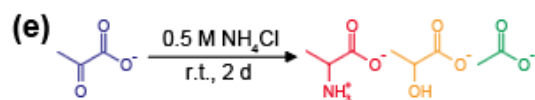


Fig. S9. (continued)

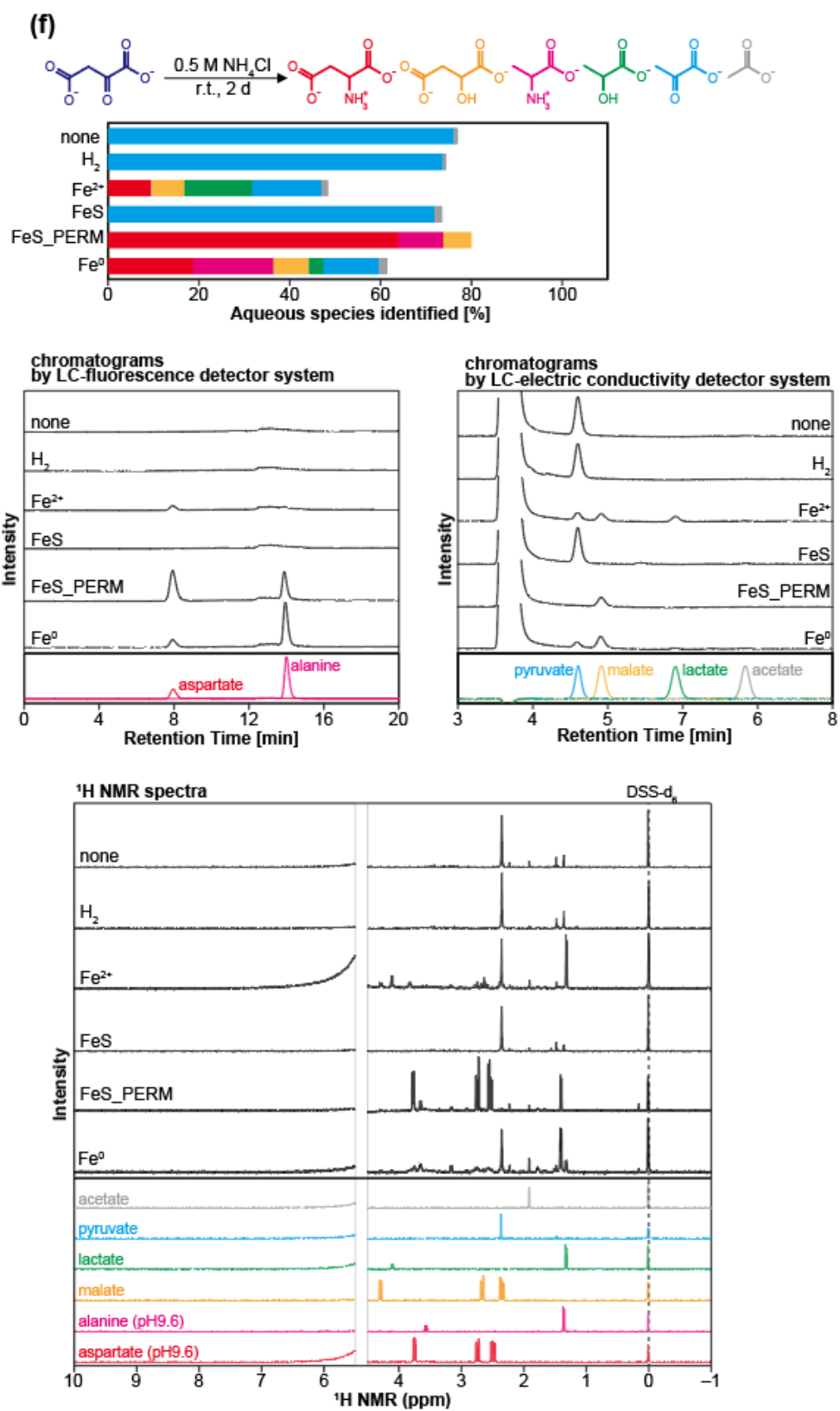


Fig. S9. (continued)

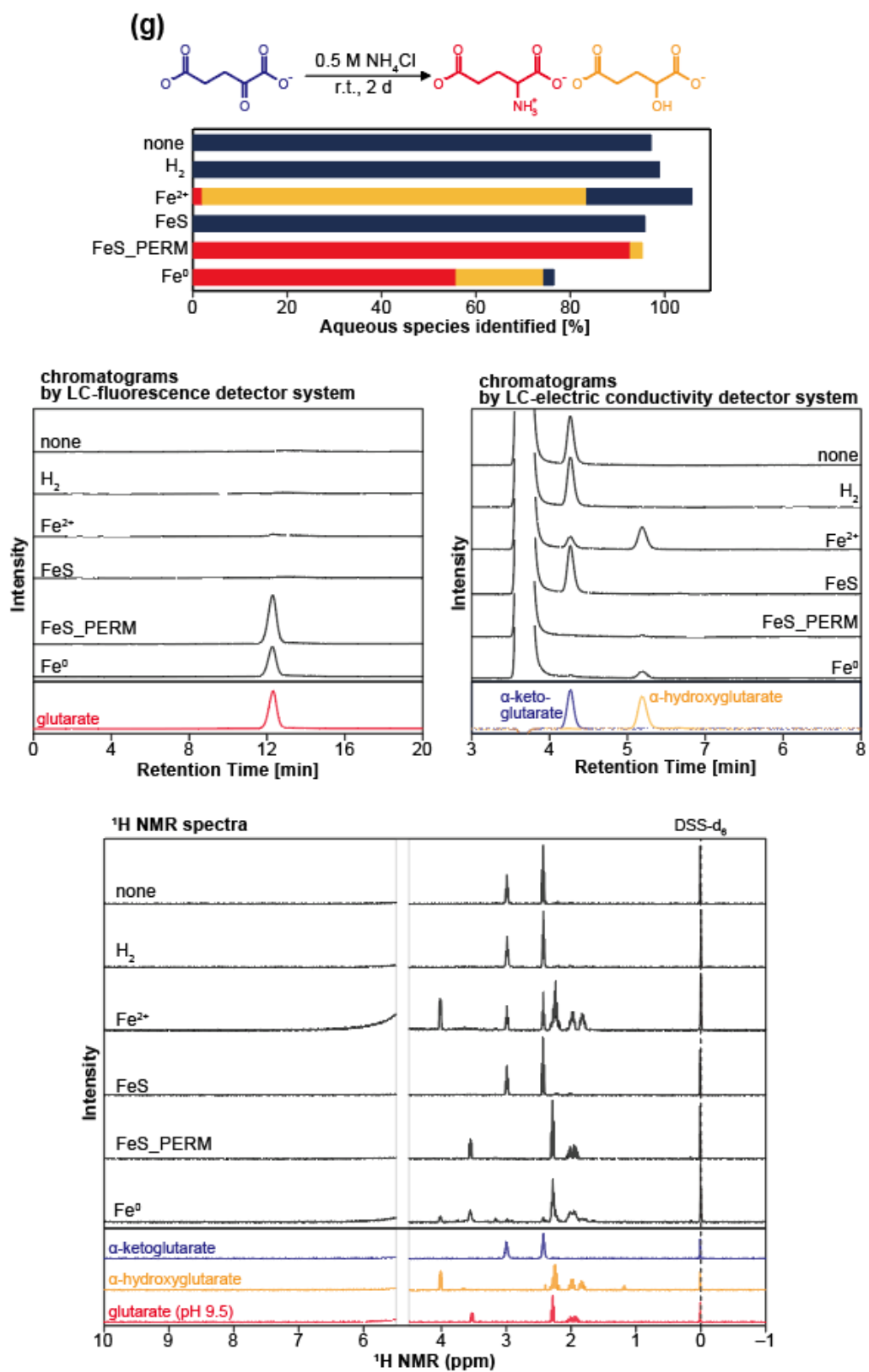


Fig. S9. (continued)

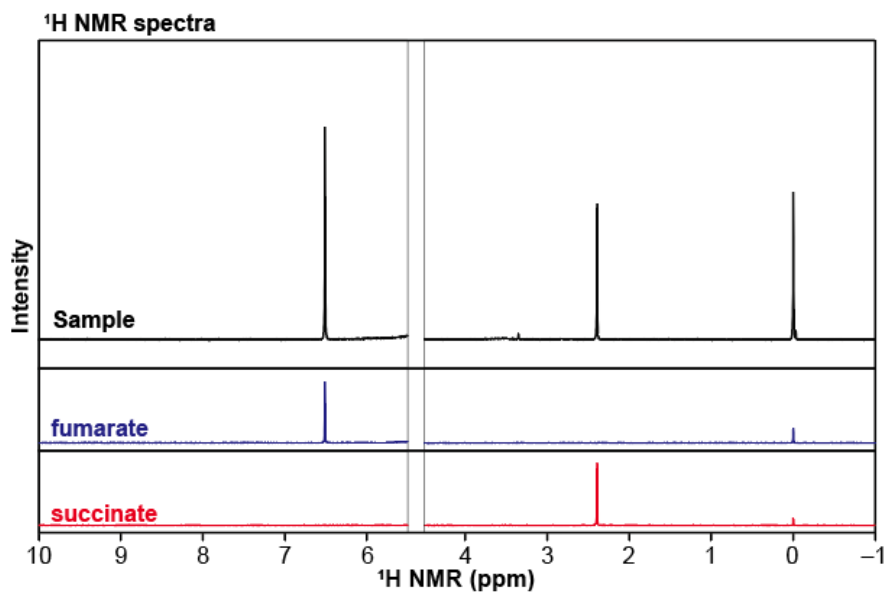
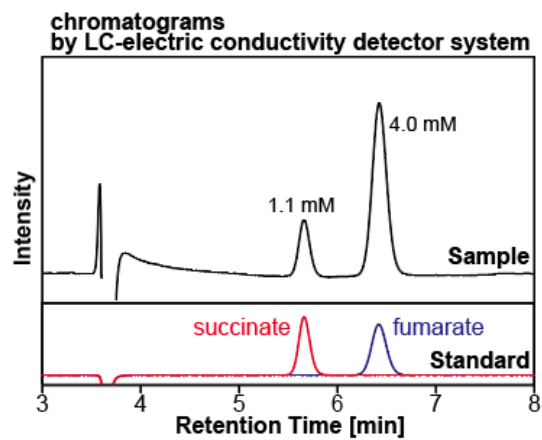
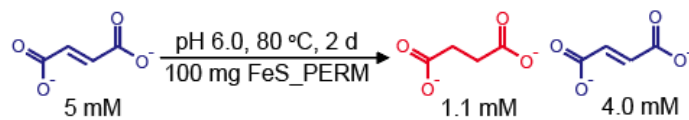


Fig. S10. Analytical results of fumarate (5 mM, 1.5 ml) incubated with the FeS_PERM (100 mg) at 80°C for 2 days.

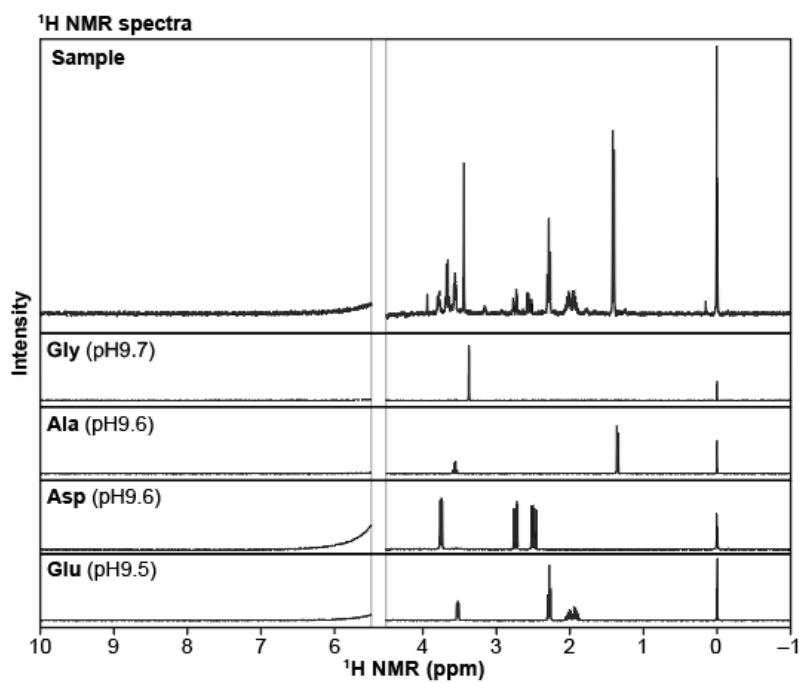
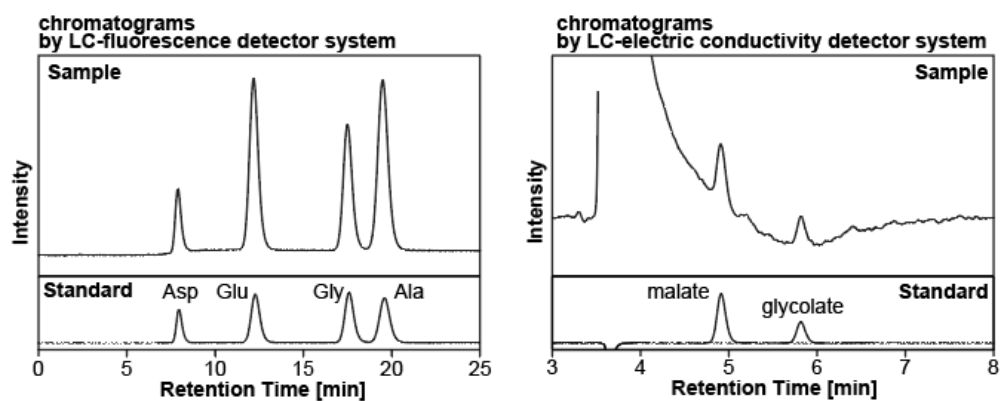
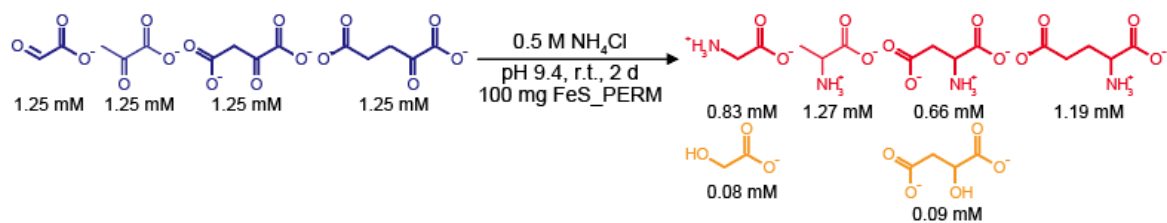


Fig. S11. Reductive amination of four keto acids promoted by the FeS_PERM in one serum bottle.

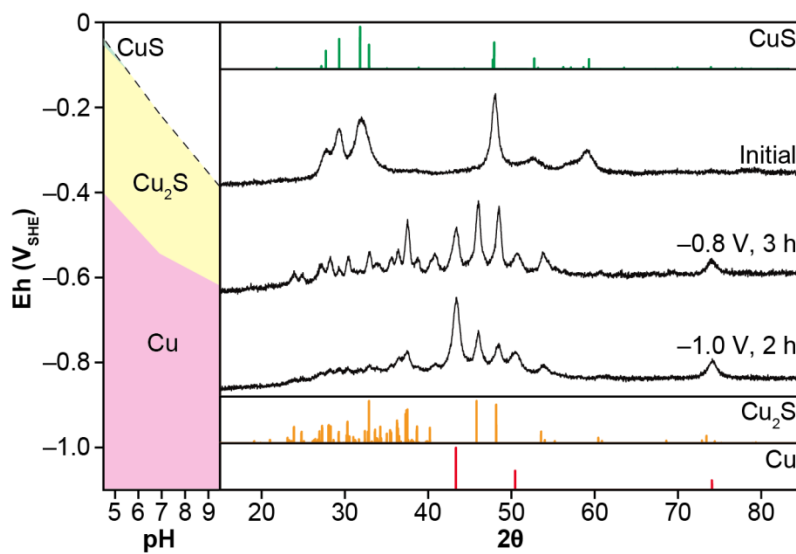


Fig. S12. XRD patterns of CuS electrolyzed at -0.8 and -1.0 V (versus SHE) for short durations.

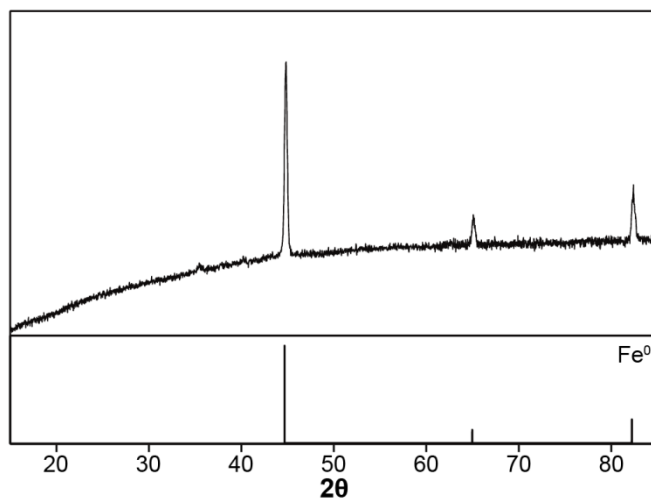


Fig. S13. XRD patterns of pure Fe⁰ used in the present study.

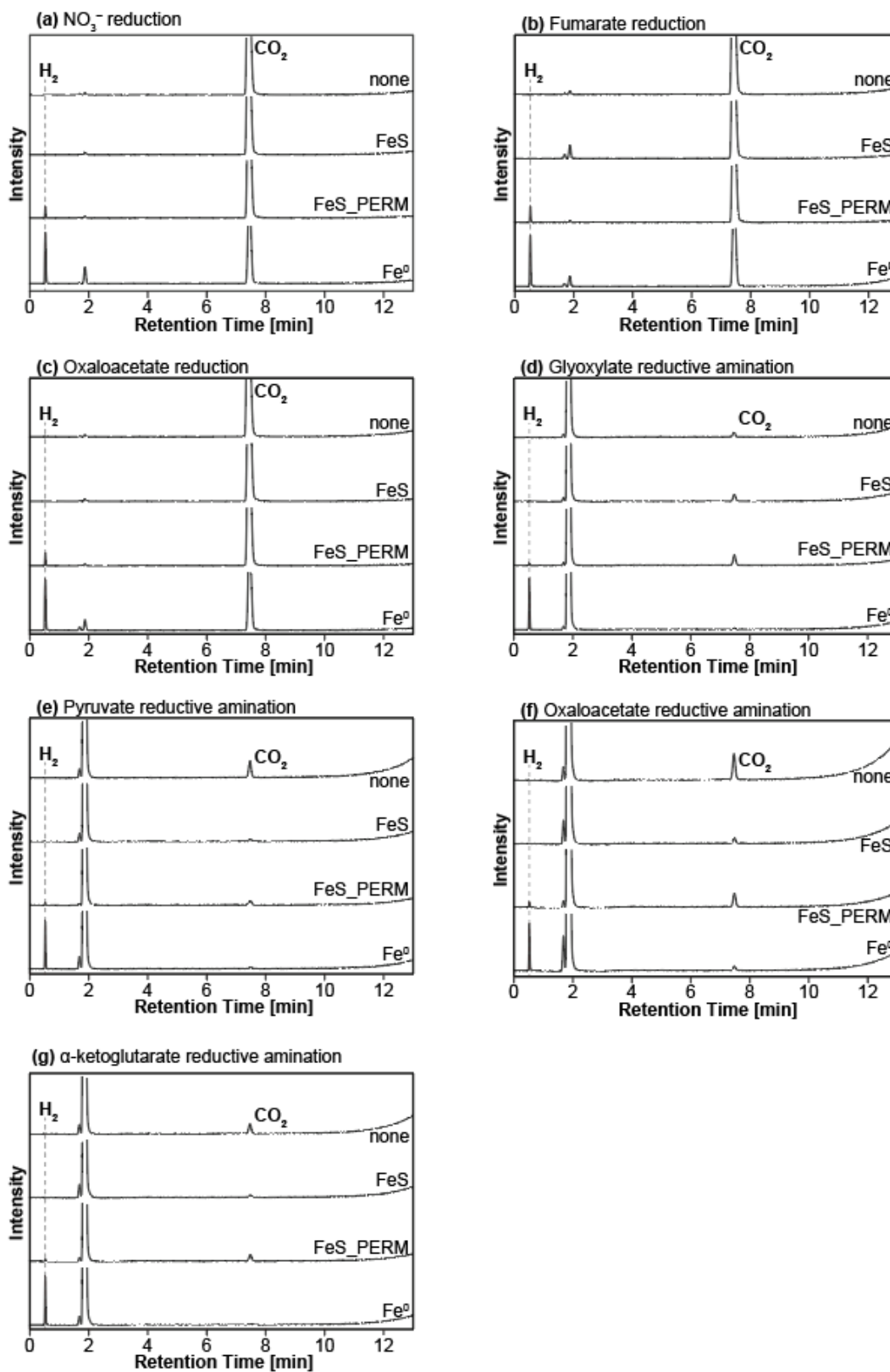


Fig. S14. GC chromatograms of the gas headspaces of serum bottles measured after the reduction experiments of organic/inorganic compounds. All chromatograms show the O₂, N₂, and CO₂ signals (partly) due to the intrusion of air into the GC system at the sample injections

Table S1. Summary of the reduction experiments of organic/inorganic compounds.(a) NO_3^- reduction ($[\text{NO}_3^-]_i = 5 \text{ mmol L}^{-1}$)

reductant	pH	NH_4^+ [mmol L ⁻¹]	NO_3^- [mmol L ⁻¹]
none	4.7	<0.01	5.03 ± 0.11
H ₂	3.0	<0.01	5.09 ± 0.25
FeCl ₂	4.5	0.07 ± 0.00	4.90 ± 0.24
FeS	6.7	0.02 ± 0.02	4.98 ± 0.01
FeS_PERM	6.5	2.94 ± 0.06	0.49 ± 0.49
Fe ⁰	6.5	5.38 ± 0.01	<0.01

(b) Oxaloacetate reduction ($[\text{Oxaloacetate}]_i = 5 \text{ mmol L}^{-1}$)

reductant	pH	Malate [mmol L ⁻¹]	Lactate [mmol L ⁻¹]	Pyruvate [mmol L ⁻¹]	Acetate [mmol L ⁻¹]
none	2.8	<0.01	<0.01	5.05 ± 0.41	0.03 ± 0.00
H ₂	2.8	<0.01	<0.01	4.81 ± 0.24	<0.01
FeCl ₂	2.8	<0.01	1.25 ± 0.06	2.34 ± 0.12	0.23 ± 0.01
FeS	6.5	<0.01	<0.01	4.22 ± 0.15	<0.01
FeS_PERM	6.4	1.83 ± 0.29	1.40 ± 0.19	0.01 ± 0.01	<0.01
Fe ⁰	6.5	<0.01	1.70 ± 0.15	0.05 ± 0.01	0.04 ± 0.00

(c) Fumarate reduction ($[\text{Fumarate}]_i = 5 \text{ mmol L}^{-1}$)

reductant	pH	Succinate [mmol L ⁻¹]	Fumarate [mmol L ⁻¹]	Malate [mmol L ⁻¹]
none	3.1	<0.01	5.06 ± 0.03	<0.01
H ₂	3.0	<0.01	5.06 ± 0.25	<0.01
FeCl ₂	2.9	<0.01	4.92 ± 0.25	<0.01
FeS	6.3	<0.01	5.01 ± 0.05	0.02 ± 0.02
FeS_PERM	6.4	0.21 ± 0.07	4.59 ± 0.02	0.02 ± 0.02
Fe ⁰	6.4	3.14 ± 0.03	0.02 ± 0.00	<0.01

(d) Glyoxylate reductive amination ($[\text{Glyoxylate}]_i = 5 \text{ mmol L}^{-1}$)

reductant	pH	Glycine [mmol L ⁻¹]	Glycolate [mmol L ⁻¹]	Glyoxylate [mmol L ⁻¹]
none	9.6	0.03 ± 0.00	<0.01	4.79 ± 0.11
H ₂	9.5	<0.01	<0.01	4.59 ± 0.23
FeCl ₂	9.1	0.33 ± 0.02	2.16 ± 0.11	0.13 ± 0.01
FeS	9.6	1.34 ± 0.06	<0.01	0.45 ± 0.07
FeS_PERM	9.6	2.97 ± 0.02	0.21 ± 0.20	0.02 ± 0.00
Fe ⁰	9.6	2.19 ± 0.04	0.38 ± 0.13	<0.01

(e) Pyruvate reductive amination ($[\text{Pyruvate}]_i = 5 \text{ mmol L}^{-1}$)

reductant	pH	Alanine [mmol L ⁻¹]	Lactate [mmol L ⁻¹]	Pyruvate [mmol L ⁻¹]	Acetate [mmol L ⁻¹]
none	9.6	<0.01	<0.01	3.90 ± 0.23	0.05 ± 0.02
H ₂	9.5	<0.01	<0.01	3.64 ± 0.18	0.03 ± 0.00
FeCl ₂	9.1	<0.01	3.70 ± 0.18	0.74 ± 0.04	<0.01
FeS	9.6	<0.01	<0.01	3.77 ± 0.11	0.07 ± 0.03
FeS_PERM	9.6	4.61 ± 0.18	<0.01	<0.01	<0.01
Fe ⁰	9.6	2.45 ± 0.01	0.55 ± 0.08	0.12 ± 0.00	<0.01

(f) Oxaloacetate reductive amination ($[\text{Oxaloacetate}]_i = 5 \text{ mmol L}^{-1}$)

reductant	pH	Aspartate [mmol L ⁻¹]	Alanine [mmol L ⁻¹]	Malate [mmol L ⁻¹]	Lactate [mmol L ⁻¹]	Pyruvate [mmol L ⁻¹]	Acetate [mmol L ⁻¹]
none	9.6	<0.01	<0.01	<0.01	<0.01	3.81 ± 0.33	0.04 ± 0.04
H ₂	9.5	<0.01	<0.01	<0.01	<0.01	3.69 ± 0.18	0.03 ± 0.00
FeCl ₂	9.0	0.46 ± 0.02	0.02 ± 0.00	0.36 ± 0.02	0.74 ± 0.04	0.76 ± 0.04	0.07 ± 0.00
FeS	9.6	<0.01	<0.01	<0.01	<0.01	3.60 ± 0.17	0.08 ± 0.03
FeS_PERM	9.6	3.20 ± 0.11	0.50 ± 0.06	0.30 ± 0.19	<0.01	<0.01	0.01 ± 0.01
Fe ⁰	9.6	0.94 ± 0.16	0.89 ± 0.02	0.39 ± 0.23	0.16 ± 0.01	0.61 ± 0.06	0.08 ± 0.00

(g) α -ketoglutarate reductive amination ($[\alpha\text{-ketoglutarate}]_i = 5 \text{ mmol L}^{-1}$)

reductant	pH	Glutamate [mmol L ⁻¹]	α -hydroxyglutarate [mmol L ⁻¹]	α -ketoglutarate [mmol L ⁻¹]
none	9.6	<0.01	<0.01	4.87 ± 0.00
H ₂	9.5	<0.01	<0.01	4.96 ± 0.25
FeCl ₂	9.0	0.10 ± 0.02	4.09 ± 0.20	1.12 ± 0.06
FeS	9.6	<0.01	<0.01	4.81 ± 0.07
FeS_PERM	9.6	4.65 ± 0.06	0.13 ± 0.10	<0.01
Fe ⁰	9.6	2.80 ± 0.09	0.93 ± 0.31	0.11 ± 0.01

Table S2. Amounts of H₂, CO, CH₄, and C₂H₆ in the serum bottles (30 ml) after the reduction experiments of organic/inorganic compounds.

(a) NO₃⁻ reduction

reductant	H ₂ [μmol]	CO [μmol]	CH ₄ [μmol]	C ₂ H ₆ [μmol]
none	<0.1	<0.01	<0.01	<0.01
FeS	<0.1	<0.01	<0.01	<0.01
FeS_PERM	58.8	<0.01	<0.01	<0.01
Fe ⁰	350.6	<0.01	0.02	<0.01

(b) Fumarate reduction

reductant	H ₂ [μmol]	CO [μmol]	CH ₄ [μmol]	C ₂ H ₆ [μmol]
none	0.2	<0.01	<0.01	<0.01
FeS	<0.1	<0.01	<0.01	<0.01
FeS_PERM	82.8	<0.01	<0.01	<0.01
Fe ⁰	348.1	<0.01	0.02	<0.01

(c) Oxaloacetate reduction

reductant	H ₂ [μmol]	CO [μmol]	CH ₄ [μmol]	C ₂ H ₆ [μmol]
none	0.1	<0.01	<0.01	<0.01
FeS	<0.1	<0.01	<0.01	<0.01
FeS_PERM	65.4	<0.01	<0.01	<0.01
Fe ⁰	356.2	<0.01	0.02	<0.01

(d) Glyoxylate reductive amination

reductant	H ₂ [μmol]	CO [μmol]	CH ₄ [μmol]	C ₂ H ₆ [μmol]
none	0.2	<0.01	<0.01	<0.01
FeS	<0.1	<0.01	<0.01	<0.01
FeS _{PEM}	4.7	<0.01	<0.01	<0.01
Fe ⁰	77.9	<0.01	<0.01	<0.01

(e) Pyruvate reductive amination

reductant	H ₂ [μmol]	CO [μmol]	CH ₄ [μmol]	C ₂ H ₆ [μmol]
none	<0.1	<0.01	<0.01	<0.01
FeS	<0.1	<0.01	<0.01	<0.01
FeS_PERM	3.3	<0.01	<0.01	<0.01
Fe ⁰	63.7	<0.01	<0.01	<0.01

(f) Oxaloacetate reductive amination

reductant	H ₂ [μmol]	CO [μmol]	CH ₄ [μmol]	C ₂ H ₆ [μmol]
none	<0.1	<0.01	<0.01	<0.01
FeS	<0.1	<0.01	<0.01	<0.01
FeS_PERM	3.3	<0.01	<0.01	<0.01
Fe ⁰	27.4	<0.01	<0.01	<0.01

(g) α-ketoglutarate reductive amination

reductant	H ₂ [μmol]	CO [μmol]	CH ₄ [μmol]	C ₂ H ₆ [μmol]
none	<0.1	<0.01	<0.01	<0.01
FeS	<0.1	<0.01	<0.01	<0.01
FeS_PERM	2.6	<0.01	<0.01	<0.01
Fe ⁰	55.5	<0.01	<0.01	<0.01

Table S3. Thermodynamic data for sulfide minerals.

Sulfide	$\Delta_f G_{P_r, T_r}^0$ [kJ/mol]	$\Delta_f H_{P_r, T_r}^0$ [kJ/mol]	S_{P_r, T_r}^0 [J/mol·K]	V_T^0 [cm ³ /mol]	$C_{P_r}^0$ [J/mol·K] ^a	refs.
Ag ₂ S, acanthite	-39.70	-32.00	142.89	34.19	75.31 (at 298.15 K)	68
CdS, greenockite	-146.10	-149.60	72.18	29.93	$35.38 + 0.01503 \times T - 533300 \times T^{-2} + 235.7 \times T^{-0.5} - 0.0000024 \times T^2$	68
CoS, jaipurite	-96.20	-95.16	58.60	16.70 ^b	$42.47 + 16.95 \times 10^{-3} T$	70
CoS ₂ , cattierite	-145.10	-150.90	74.80	25.52	$65.82 + 0.03032 \times T - 587000 \times T^{-2}$	68
Co ₃ S ₄ , linnaeite	-334.90	-347.50	176.00	62.55	–	68
Co ₉ S ₈ , cobaltpentlandite	-834.69 ^c	-851.40	470.70	147.10 ^d	$362 + 0.14 \times T$	70
CuS, covellite	-55.30	-54.60	67.40	20.42	$43.049 + 0.02023 \times T - 139938 \times T^{-2} + 0.435838 \times T^{-0.5}$	68
Cu _{1.75} S, anilite	-78.50	-73.30	107.50	25.79	–	68
Cu _{1.80} S, digenite	-78.30	-73.00	109.60	25.63	–	68
Cu _{1.95} S, djurleite	-84.20	-78.80	114.80	26.89	–	68
Cu ₂ S, chalcocite	-89.20	-83.90	116.20	27.48	76.84 (at 298.15 K)	68
FeS, mackinawite	-100.07	-100.85 ^c	56.52	18.20 ^f	$44.685 + 0.019037 \times T - 289000 \times T^{-2}$	71
FeS, troilite	-102.90	-102.60	60.30	18.20	50.49 (at 298.15 K)	68
Fe _{0.875} S, pyrrhotite	-98.90	-97.50	60.70	17.49	49.88 (at 298.15 K)	68
Fe ₃ S ₄ , greigite	-311.88	-320.03	182.13	72.499 ^g	$143.344 + 0.076567 \times T$	71
FeS ₂ , pyrite	-160.10	-171.50	52.90	23.94	$-20.32 + 0.0503 \times T - 320000 \times T^{-2} + 1787 \times T^{-0.5}$	68
FeS ₂ , marcasite	-158.40	-169.50	53.90	24.58	$383.2 - 0.3173 \times T + 1676000 \times T^{-2} - 4488 \times T^{-0.5} + 0.0001676 \times T^2$	68
MnS, alabandite	-218.70	-213.90	80.30	21.46	$135.3 - 0.05775 \times T + 1169000 \times T^{-2} - 1435 \times T^{-0.5} + 0.00002087 \times T^2$	68
MnS ₂ , hauerite	-224.60	-223.80	99.90	34.20	–	68
MoS ₂	-267.14 ^h	-276.14	62.57	31.63 ^b	$71.67318 + 7.515343 \times t - 0.044947 \times t^2 + 0.008866 \times t^3 - 0.921212 \times t^{-2}$	69
MoS ₃	-295.24 ^h	-310.00	75.30	37.97 ⁱ	–	70
Mo ₂ S ₃	-395.62 ^h	-407.10	114.98	49.50 ^j	$110.2911 + 32.96866 \times t + 0.000664 \times t^2 - 0.000106 \times t^3 - 0.962354 \times t^{-2}$	69
NiS, millerite	-88.30	-91.00	52.97	16.89	47.11 (at 298.15 K)	68
Ni ₃ S ₂ , heazlewoodite	-210.20	-216.30	133.20	40.95	$1057 - 0.8988 \times T + 8139000 \times T^{-2} - 13880 \times T^{-0.5} + 0.000466 \times T^2$	68
NiS ₂ , vaesite	-124.82 ^k	-131.38	71.96	27.688 ^g	$64.4336 + 20.76331 \times t - 0.009134 \times t^2 + 0.002569 \times t^3 + 0.000227 \times t^{-2}$	69
Ni ₃ S ₄ , polydemite	-291.78 ^k	-301.12	186.48	64.326 ^g	$121.9707 + 143.6585 \times t + 0.025374 \times t^2 - 0.01786 \times t^3 + 0.000434 \times t^{-2}$	69
PbS, galena	-96.80	-98.30	91.70	31.49	$44.6 + 0.0164 \times T$	68
WS ₂ , tungstenite	-233.00	-241.60	67.80	32.07	$76.33 + 0.0005561 \times T - 1137000 \times T^{-2} + 0.000001408 \times T^2$	68
WS ₃	-277.68	-293.00	77.40	36.85 ^l	–	70
ZnS, sphalerite	-199.60	-204.10	58.70	23.83	$61.51 + 0.0007631 \times T - 79630 \times T^{-2} - 260.4 \times T^{-0.5}$	68
ZnS, wurtzite	-199.40	-203.80	58.80	23.85	$41.91 + 0.0007619 \times T - 660300 \times T^{-2} + 157.7 \times T^{-0.5}$	68

^a T = temperature [K], t = T × 10⁻³.^b ref. (73).^c calculated using the values of $\Delta_f H^0$ and S^0 listed in the table together with the standard molar entropies of Co and S reported by ref. (68).

^d ref. (72).

^e calculated using the values of $\Delta_f G^\circ$ and S° listed in the table together with the standard molar entropies of Fe and S reported by ref. (68).

^f assumed to be the same as that of troilite.

^g ref. (75).

^h calculated using the values of $\Delta_f H^\circ$ and S° listed in the table together with the standard molar entropies of Mo and S reported by ref. (68).

ⁱ calculated using the density value for MoS_2 reported by ref. (73).

^j ref. (74).

^k calculated using the values of $\Delta_f H^\circ$ and S° listed in the table together with the standard molar entropies of Ni and S reported by ref. (68).

^l calculated using the density value for WS_2 reported by ref. (73).